Workshop on Visualisation in Environmental Sciences (EnvirVis) (2016)
A. Middel, K. Rink, and D. Zeckzer (Editors)

Visual Analysis of Reservoir Simulation Ensembles

Thomas Höllt[1,2] Fabio Miguel de Matos Ravanelli,[3] Markus Hadwiger[2] Ibrahim Hoteit[2]

[1]Computer Graphics and Visualization, TU Delft, The Netherlands
[2]King Abdullah University of Science and Technology, Saudi Arabia
[3]Saudi Aramco, Saudi Arabia

Abstract

Hydrocarbon reservoir simulation models produce large amounts of heterogeneous data, combining multiple variables of different dimensionality, such as two or three-dimensional geospatial estimates with abstract estimates simulated for the complete field or different wells. In addition these simulations are nowadays often run as so-called ensemble simulations, to capture uncertainty of the model, as well as boundary conditions as variation in the output. The (visual) analysis of such data is a challenging process, due to the size and complexity of the data. In this paper we present an integrated system for the visual analysis of ensemble reservoir simulation data. We provide tools to inspect forecasts for multiple variables of complete fields, as well as different wells. Finally, we present a case study highlighting the effectiveness of the presented system.

Categories and Subject Descriptors (according to ACM CCS): I.3.8 [Computer Graphics]: Applications—

1. Introduction

Ensemble forecasts, i.e., simulations that result in multi-valued, multi-variate, and multi-dimensional data, are computed in many different application areas, such as the geo-sciences. Numerical models are limited by computational resources and, as such, are not exact. Additionally, starting conditions and model inputs (e.g. forcing and parameters) are often not well known due to scarcity of data and measurement errors. The inherent uncertainty can be mapped to multiple runs of the same or of different models, resulting in multiple possible outcomes forming an ensemble representing the probability distribution of the simulated fields. Most notable applications for ensemble simulations are weather and climate forecasts, where such data are the de-facto standard. However, similar data becomes relevant in basically all geophysical simulations, such as ocean forecasting [HPB02,HHG*13] or, recently, also in petroleum engineering applications [ANO*09,KASH15,KHS15]. While similar in spirit, such reservoir simulations combine different types of data and pose different requirements to the analysis process compared to the more widely used weather or climate forecasts.

Specifically, in the application, presented here, we combine unstructured 4D spatio-temporal data, containing multiple variables such as pressure or water saturation for each grid cell of the simulated reservoir with one dimensional temporal data of production rate forecasts at single wells as well as the complete field. Besides the pure data exploration, comparison of different data points is crucial. E.g., one might ask how production rates that were simulated for different possible well positions compare. We propose the use of a multiple-linked-views [Rob07] framework for the exploration and analysis of these data.

2. Related Work

While the display of uncertainty information, such as error bars, are ubiquitous in visualization of abstract data for a while now, it is a relatively new development to present this information to the user of visualizations in a spatial context. Pang et al. [PWL97] present an overview of early work on uncertainty visualization for scientific 3D data. Later, Johnson and Sanderson challenge the visualization community *"to take the next step and make visually representing errors and uncertainties the norm rather than the exception"* [JS03]. This call is not an ends to itself. In many fields data containing uncertainty information has become ubiquitous in recent years, especially in the area of numerical simulations, where ensemble simulations are the norm ([KDP01, LKP03, KKL*05, LPK05]). Weather and climate forecasts are on the forefront of this development, justifying the development of several fully featured ensemble visualiation applications, such as *Ensemble-Vis* by Potter et al. [PWB*09], *Noodles* by Sanyal et al. [SZD*10] or *Met.3D* by Rautenhaus et al. [RKSW15]. Similarly, systems for ocean forecasts (i.e. *OVis* by Höllt et al. [HMC*13, HMZ*14]) and storm surge predictions [HAM*15] were presented recently. Köthur et al. [KWS*15] present a general approach to the visual analysis of time series ensembles. All of these tools use multiple views on the data, some show aggregates of the multivalued part of the ensemble, for example by means of statistics, while other views let the user directly compare different results. Examples for comparative approaches to ensemble visualization in various application areas are the works of Healey and Snoeyink [HS06], Matković et al. [MGKH09], Piringer et al. [PPBT12], or Demir et al. [DDW14]. Whitaker et al. introduced an implementation of boxplots for contours [WMK13] and generalized it for curves [MWK14].

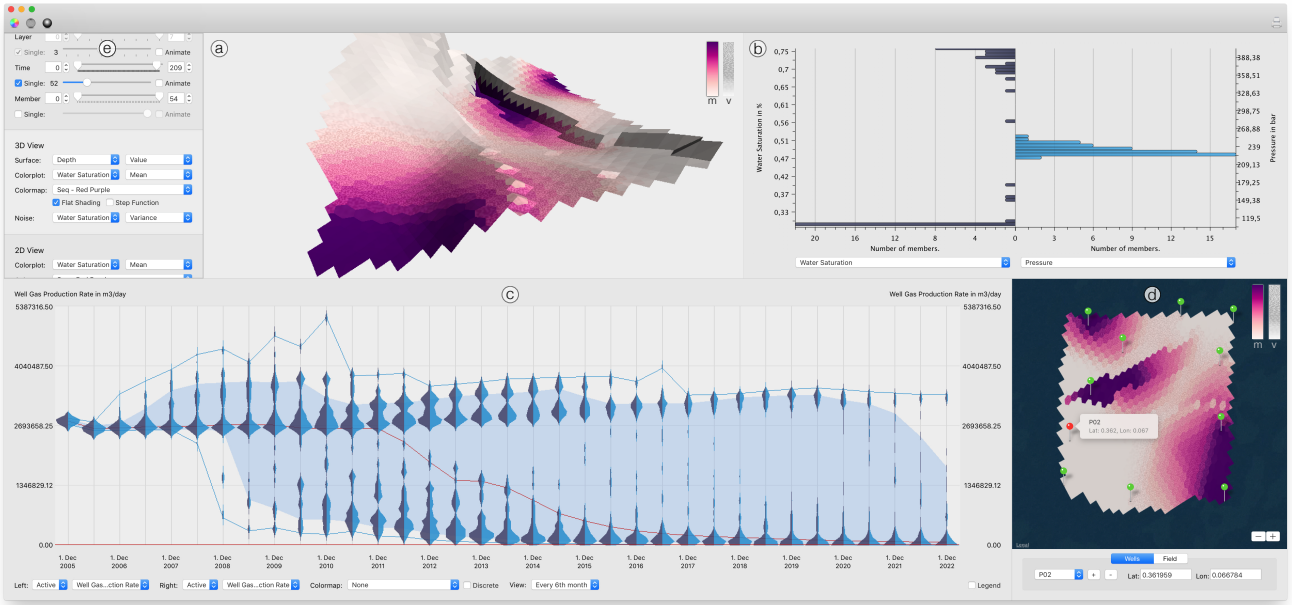

Figure 1: **System Overview.** A screenshot of the presented application, showing the combination of different views: a 3D view of a single layer of the reservoir (a), showing the reservoir geometry in combination with water saturation mean and variance. b shows the complete distribution of all members of the ensemble for two variables (here water saturation and pressure) for a single selected point in space and time. c shows a prediction of oil and gas production rates for a selected production well over 18 years. d shows a 2D version of a plus the position of the selected well.

3. Visual Analysis System

We show a screenshot of our proposed visual analysis system in Figure 1. The presented system is based on the ocean forecast visualization system *OVis* [HMZ*14] that was adapted to the specific requirements for the reservoir analysis. The system is divided into four data views (Figure 1a-d) plus a unified settings widget (Figure 1e). The views adapt flexibly to the data and can be configured to show any available data. We refer to the supplemental video for an interactive impression of the system.

Figure 1a shows a 3D visualization of a single layer of the reservoir. While the data is three-dimensional, depth is not a continuos axis, but is rather divided into a few discrete layers, each consisting of complex 3D geometry. We decided to show only one of these layers at a time, since multiple layers would be mostly occluded by the top layer. Instead we provide a simple slider that allows the user to sweep through all available layers. In total the view provides three channels to visualize different variables of the data: geometry, color and noise. In the standard setting the geometry of the surface represents the actual geometry of the reservoir. The underlying grid is being provided as an unstructured mesh. We use color coding to show the mean value of a given variable, such as water saturation. To indicate uncertainty, we added the possibility to blend a noise texture with variable frequency on top of the color plot to show standard deviation or variance (see detail in Figure 2). We use a smooth transition from no noise through low frequency noise to high frequency noise to indicate increasing variance or standard deviation values. Figure 2a shows the combination of color mapping the mean and using the noise overlay to show the variance. Figure 2b shows only the variance using noise. For illustration we show the variance using color mapping in Figure 2c.

In addition to the described standard settings we compute a number of statistics, such as the median or higher order moments on demand, that can be assigned to any of the visual channels. It is also possible to select specific ensemble members or combine different variables to find correlations and dependencies. The user can probe in the 3D view, by hovering the mouse over any position, and we show the complete distribution of selected variables of the ensemble in the attached histogram view (Figure 1b).

The 2D view, as presented in Figure 1d provides the same functionality as the 3D view, with the exception of 3D geometry. In addition the 2D view provides a visualization of the positions of loaded wells, represented by needles. The user can load these positions from file, including separate data, such as the oil production for a production well or the water injection rate for an injection well, or interactively define positions to probe the data available on the grid within the application.

Figure 1b shows the comparative histogram view. We show two histograms for comparing the distributions of two different variables and/or positions. The histograms x- and y-axis are flipped, compared to the conventional histogram, where the x-axis is usually used for the variable and the y-axis for the number of occurrences. The y-axis is shared, with the left histograms' x-axis pointing to the left and the right histograms x-axis to the right. This configuration is specifically suited for comparison of two distributions. While the horizontal orientation is much more common

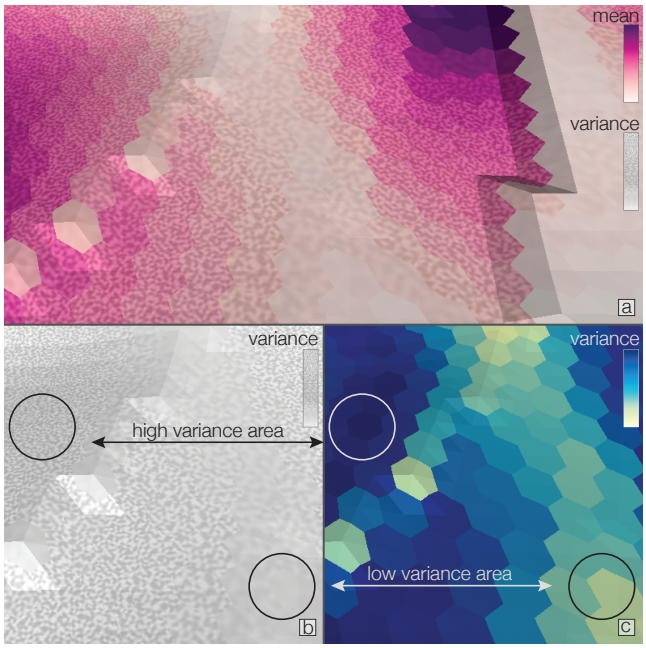

Figure 2: **Visualization of Variance by a Noise Overlay.** We use a combination of color mapping and noise overlay to show two variables at once (a). b shows the noise overlay for the variance of a cut out of a, without color mapping a second variable. Low frequency noise corresponds to little variance, high frequency noise strong variation (see highlighted areas in b and c). For illustration we use color mapping to show the variance in the same area in c.

for histograms we found out that for comparison this configuration works very well. The two sides of the histogram view can be freely configured to show any of the available variables. The main idea is to show the detailed distribution of the two- or three-dimensional variables at a single grid point. Therefore, the user can select the desired position by simply hovering the mouse over the surface in the 3D view. In an alternative mode positions can also be picked. E.g., the user can select a fixed position for one side of the histogram and show the histogram for the position where the mouse hovers on the other side, for comparison. The histogram updates in real-time when the user moves the mouse, allowing for very fast probing of the data. Alternatively the user can also select different variables (at the same or different positions) for the different sides of the histogram to inspect the interplay of different variables.

We extend the idea of the histogram view in the time series view (Figure 1c). Based on the two-sided histogram we use a simple glyph (Figure 4b), as introduced by Höllt et al. [HMZ*14]. The histogram is smoothed using kernel density estimates and the resulting estimate of the probability density function (pdf) is used as the contour of the glyph. Just as the histogram view the glyph can be configured to show the pdf of different variables and/or positions on the two sides. Glyphs for each simulated time point are then arranged on the x-axis of the time series view. In the example in Figure 1c we show the oil and gas production rate, respectively, for a selected well using the two sides of the glyphs. The example demonstrates the need for such a detailed view of the ensemble distribution, instead of simply using mean and variance. After the first few time steps the glyphs become very elongated, indicating large uncertainty. However, the distributions are multi-modal and can not easily be parametrized, such as a Gaussian distribution.

The time series in these data consist of many more time steps, than the ocean forecasts presented in prior work [HMZ*14]. The example shown in Figure 1 consists of 216 time steps, representing monthly samples of 18 years. Using finer sampling or an even larger time span would rapidly increase the data size. To adapt the time series view to these larger time series we implemented a summary overview visualization, as well as filtering of the time series. To summarize the time series statistics we use a simple connected box-plot (Figure 4). For each time step we compute the median, 10th and 90th percentile, as well as the minimum and maximum values. We show the median and extrema as lines, connecting each time step in the time series. The area between the 10th and 90th percentile is filled semi-transparently using the same color hue that is used for the glyph. Showing all time steps of a large time series using the glyph-based visualization results in a lot of clutter and is limited by available screen real estate. The box-plot allows us to filter the glyphs, without losing too much information. Therefore, we provide the user with the option to select an appropriate sampling of the glyphs. One way to do this is by simply selecting every n-th time step. We also provide a smart sampling, based on an automatic analysis of the original temporal resolution of the time series. E.g., assuming a temporal resolution of one day, we allow weekly and monthly filtering. This filtering is based on the calendar, so e.g., monthly filtering results in non uniformly sized time steps of 28–31 days. We also apply this filtering in case of missing data, or if the temporal domain itself has been sampled non-uniformly.

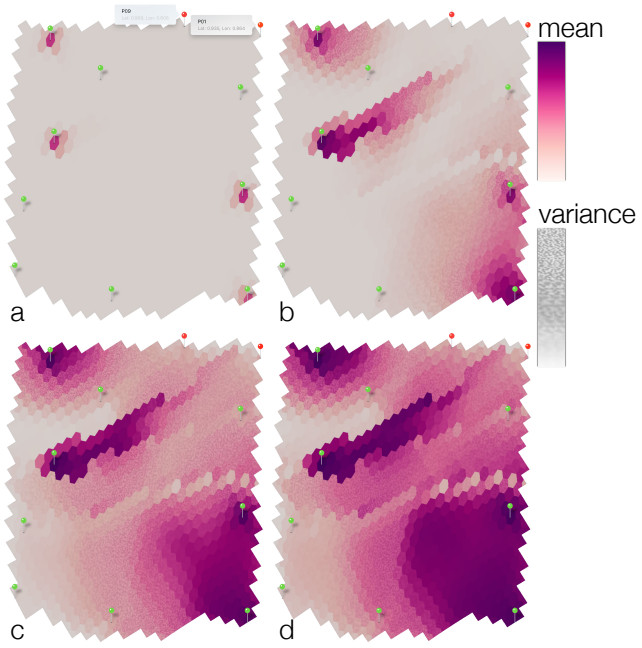

Figure 3: **Illustration of the Spatial Analysis** for injection well placement. It becomes apparent that large parts on the left side of the reservoir are not swept when injecting water.

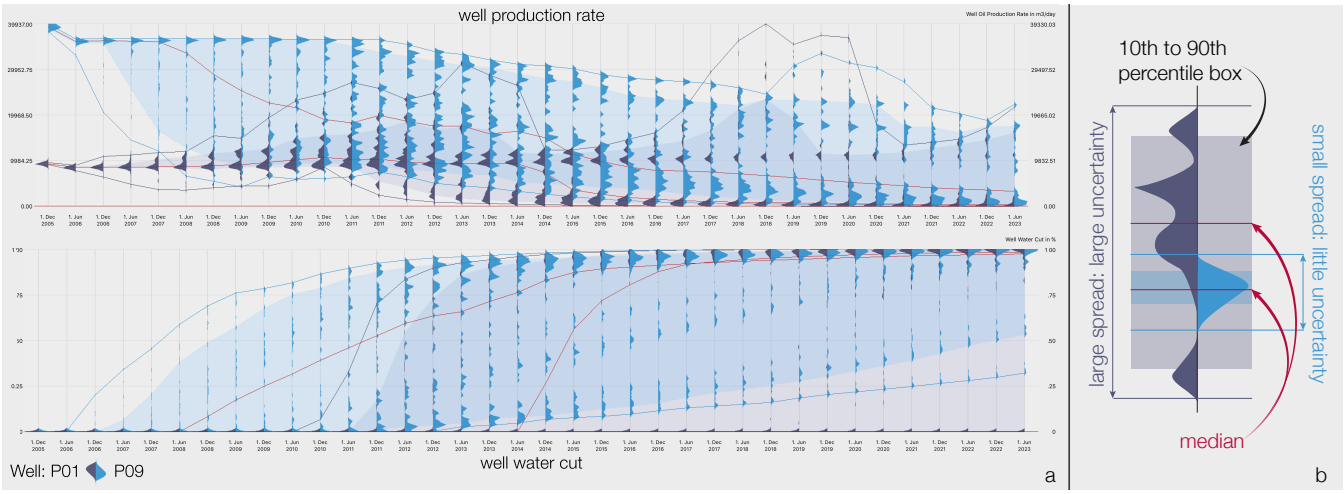

Figure 4: **Illustration of the Time Series Analysis** for injection well placement. The top view in a shows a comparison of the well production rate over time for two wells, P01 and P09. The bottom shows the water cut rate. The components of the glyph are described in b.

4. Use Case

We present a use case of a real world reservoir forecast analysis, using the presented system. We use a forecast dataset that was computed using a multi-data Ensemble Kalman-based history matching framework, as presented by Katterbauer et al. [KASH15]. The forecast consists of a time series of monthly samples of 18 years, between January 2006 and December 2023, resulting in 216 time steps. Each time step consists of multiple, unstructured 3D scalar fields, including water saturation, pressure, permeability, and (temporally stable) rock porosity, covering the complete reservoir domain. Each 3D field is composed of eight horizontal layers, consisting of 5800 grid cells, each. In addition to the spatial data the dataset includes field predictions and 11 wells, seven oil producers and four injection wells. Oil, water and gas production rates, as well as the water cut are predicted for individual producer wells as well as the cumulative rates and field level performance. Borehole pressure is forecasted at all wells. In addition, injection well forecasts include water injection rates. Simulated results are available for each of the 55 geological realizations present in this ensemble to account for geological and engineering uncertainties in the model.

A typical reservoir management study consists of proposing infill well locations and recommending production strategies, to maximize sweep efficiency of the reservoir and thus increasing the net present value of the asset. Figure 3 shows several samples of the water saturation of the top layer of the reservoir over time (timesteps 5, 60, 120 and 180 are shown in Figure 3a-d, respectively). In the presented application one could simply scrub the time slider to get to these points in the time series. Naturally the water saturation increases first in the areas around the injection wells (Figure 3a). In the following time steps it becomes clear that water injected through the two wells in the bottom right merges very early (Figure 3b/c) and creates a highly saturated area in the lower right corner of the reservoir and finally that the saturation in the lower left area remains rather low even very late in the time series.

Figure 4 shows two different time series plots for the production wells P01 and P09, highlighted in Figure 3a. Solely based on the visualization in Figure 3, the water saturation over time seems to be quite similar for these two positions. Thus, without the time series view (Figure 4) we would also expect similar production rates for these two positions. The detail analysis, however, reveals a much more complex situation. The top time series in Figure 4a shows the oil production, the bottom time series shows the water cut. Oil production at P09 is expected to be much higher, compared to P01 from the beginning. However, the much larger spread in the blue part of the glyphs, corresponding to P09, also indicates a much larger uncertainty and as such a higher risk that the well will not perform as expected. Contrary, the plots for P01 exhibit much less variation and as such less uncertainty. Looking at the time series for the water cut (Figure 4a, bottom) we see that the water cut for P09 increases much earlier compared to P01 and also with a much flatter curve. That would put a large economical burden on production from this well, as oil and water needs to be separated from early on. The combination of these two series show the complex decision making process to decide on well placement. P09 initially exhibits much higher production rates, however, at higher uncertainty and the economical benefit of these might greatly be diminished by a costly process of reducing the water cut. With our tool the analyst can make an informed decision based on all available data.

5. Conclusion

In this work, we present an interactive system for the visual exploration and analysis of reservoir forecasts based on ensemble simulation. The system extends and adapts previous work for the visualization of ocean forecasts to support the specific needs for the analysis of reservoir forecasts. We show how our tool supports the complex decision making process in a simple use case.

For the future we would like to use the system to steer the optimal field development planning. One could think of defining possible positions for well placement and based on this run the reservoir simulator again, to investigate the possible well potential and likelihood of success. The newly created forecasts could then be compared directly with the results of the previous forecasts, using the presented tools.

Acknowledgements. We would like to thank the anonymous reviewers for their constructive criticism. Research reported in this publication was supported by the King Abdullah University of Science and Technology (KAUST).

References

[ANO*09] AANONSEN S. I., NÆVDAL G., OLIVER D. S., REYNOLDS A. C., VALLÈS B.: The ensemble kalman filter in reservoir engineering–a review. *SPE Journal 14*, 3 (2009), 393–412. doi:10.2118/117274-PA. 1

[DDW14] DEMIR I., DICK C., WESTERMANN R.: Multi-charts for comparative 3d ensemble visualization. *IEEE Transactions on Visualization and Computer Graphics 20*, 12 (2014). doi:10.1109/TVCG.2014.2346448. 1

[HAM*15] HÖLLT T., ALTAF M., MANDLI K., HADWIGER M., DAWSON C., HOTEIT I.: Visualizing uncertainties in a storm surge ensemble data assimilation and forecasting system. *Natural Hazards 77*, 1 (2015), 317 – 336. doi:10.1007/s11069-015-1596-y. 1

[HHG*13] HOTEIT I., HOAR T., GOPALAKRISHNAN G., ANDERSON J., COLLINS N., CORNUELLE B., KÖHL A., HEIMBACH P.: A MITgcm/DART ensemble analysis and prediction system with application to the gulf of mexico. *Dynamics of Atmospheres and Oceans 63* (2013), 1–23. doi:10.1016/j.dynatmoce.2013.03.002. 1

[HMC*13] HÖLLT T., MAGDY A., CHEN G., GOPALAKRISHNAN G., HOTEIT I., HANSEN C. D., HADWIGER M.: Visual analysis of uncertainties in ocean forecasts for planning and operation of off-shore structures. In *Proceedings of the IEEE Pacific Visualization Symposium* (2013), pp. 59–66. doi:10.1109/PacificVis.2013.6596144. 1

[HMZ*14] HÖLLT T., MAGDY A., ZHAN P., CHEN G., GOPALAKRISHNAN G., HOTEIT I., HANSEN C. D., HADWIGER M.: Ovis: A framework for visual analysis of ocean forecast ensembles. *IEEE Transactions on Visualization and Computer Graphics 20*, 8 (2014), 1114–1126. doi:10.1109/tvcg.2014.2307892. 1, 2, 3

[HPB02] HOTEIT I., PHAM D.-T., BLUM J.: A simplified reduced order Kalman filtering and application to altimetric data assimilation in Tropical Pacific. *Journal of Marine Systems 36* (2002), 101–127. doi:10.1016/S0924-7963(02)00129-X. 1

[HS06] HEALEY C. G., SNOEYINK J.: VisTRE: A visualization tool to evaluate errors in terrain representation. In *Proceedings of the Third International Symposium on 3D Data Processing, Visualization, and Transmission* (2006), pp. 1056–1063. doi:10.1109/3DPVT.2006.146. 1

[JS03] JOHNSON C. R., SANDERSON A. R.: A next step: Visualizing errors and uncertainty. *IEEE Computer Graphics and Applications 23*, 5 (2003), 6–10. doi:10.1109/MCG.2003.1231171. 1

[KASH15] KATTERBAUER K., ARANGO S., SUN S., HOTEIT I.: Multi-data reservoir history matching for enhanced reservoir forecasting and uncertainty quantification. *Journal of Petroleum Science and Engineering 128* (2015), 160–176. doi:10.1016/j.petrol.2015.02.016. 1, 4

[KDP01] KAO D. L., DUNGAN J. L., PANG A. T.: Visualizing 2D probability distributions from EOS satellite image-derived data sets: a case study. In *Proceedings of the IEEE Visualization Conference* (2001), pp. 457–560. doi:10.1109/VISUAL.2001.964550. 1

[KHS15] KATTERBAUER K., HOTEIT I., SUN S.: History matching of electromagnetically heated reservoirs incorporating full-wavefield seismic and electromagnetic imaging. *SPE Journal 20*, 5 (2015), 923–941. doi:10.2118/173896-PA. 1

[KKL*05] KAO D. L., KRAMER M., LOVE A. L., DUNGAN J., PANG A. T.: Visualizing distributions from multi-return lidar data to understand forest structure. *The Cartographic Journal 42*, 1 (2005), 35–47. doi:10.1179/000870405X57257. 1

[KWS*15] KÖTHUR P., WITT C., SIPS M., MARWAN N., SCHINKEL S., DRANSCH D.: Visual analytics for correlation-based comparison of time series ensembles. *Computer Graphics Forum 34*, 3 (2015), 411–420. doi:10.1111/cgf.12653. 1

[LKP03] LUO A., KAO D. L., PANG A. T.: Visualizing spatial distribution data sets. In *Proceedings of the Symposium on Data Visualisation* (2003), pp. 29–38. doi:10.2312/VisSym/VisSym03/029-038. 1

[LPK05] LOVE A. L., PANG A. T., KAO D. L.: Visualizing spatial multivalue data. *IEEE Computer Graphics and Applications 25*, 3 (2005), 69–79. doi:10.1109/MCG.2005.71. 1

[MGKH09] MATKOVIĆ K., GRACANIN D., KLARIN B., HAUSER H.: Interactive visual analysis of complex scientific data as families of data surfaces. *IEEE Transactions on Visualization and Computer Graphics 15*, 6 (2009), 1351–1358. doi:10.1109/TVCG.2009.155. 1

[MWK14] MIRZARGAR M., WHITAKER R. T., KIRBY R. M.: Curve boxplot: Generalization of boxplot for ensembles of curves. *IEEE Transactions on Visualization and Computer Graphics 20*, 12 (Dec 2014). doi:10.1109/TVCG.2014.2346455. 1

[PPBT12] PIRINGER H., PAJER S., BERGER W., TEICHMANN H.: Comparative visual analysis of 2d function ensembles. *Computer Graphics Forum 31*, 3 (2012), 1195–1204. doi:10.1111/j.1467-8659.2012.03112.x. 1

[PWB*09] POTTER K., WILSON A., BREMER P.-T., WILLIAMS D., DOUTRIAUX C., PASCUCCI V., JOHNSON C. R.: Ensemble-Vis: A framework for the statistical visualization of ensemble data. In *IEEE Workshop on Knowledge Discovery from Climate Data: Prediction, Extremes and Impacts* (2009), pp. 233–240. doi:10.1109/ICDMW.2009.55. 1

[PWL97] PANG A. T., WITTENBRINK C. M., LODHA S. K.: Approaches to uncertainty visualization. *The Visual Computer 13* (1997), 370–390. doi:10.1007/s003710050111. 1

[RKSW15] RAUTENHAUS M., KERN M., SCHÄFLER A., WESTERMANN R.: Three-dimensional visualization of ensemble weather forecasts – part 1: The visualization tool met.3d (version 1.0). *Geoscientific Model Development 8*, 7 (2015), 2329–2353. doi:10.5194/gmd-8-2329-2015. 1

[Rob07] ROBERTS J. C.: State of the art: Coordinated multiple views in exploratory visualization. In *Fifth International Conference on Coordinated and Multiple Views in Exploratory Visualization (CMV)* (2007), pp. 61–71. doi:10.1109/CMV.2007.20. 1

[SZD*10] SANYAL J., ZHANG S., DYER J., MERCER A., AMBURN P., MOORHEAD R. J.: Noodles: A tool for visualization of numerical weather model ensemble uncertainty. *IEEE Transactions on Visualization and Computer Graphics 16*, 6 (2010), 1421 – 1430. doi:10.1109/TVCG.2010.181. 1

[WMK13] WHITAKER R. T., MIRZARGAR M., KIRBY R. M.: Contour boxplots: A method for characterizing uncertainty in feature sets from simulation ensembles. *IEEE Transactions on Visualization and Computer Graphics 19*, 12 (2013), 2713–2722. doi:10.1109/TVCG.2013.143. 1